BNL-228054-2025-TECH
EIC-ADD-TN-119

Direct determination of the temperatures of the Carbon targets at the CNI polarimeters in RHIC when hit by the proton beam

V. Shmakova

April 2025

Electron-Ion Collider

Brookhaven National Laboratory

U.S. Department of Energy

USDOE Office of Science (SC), Nuclear Physics (NP)

DISCLAIMER

Direct determination of the temperatures of the Carbon targets at the CNI polarimeters in RHIC when hit by the proton beam

Vera Shmakova, Prashanth Shanmuganathan, Frank Rathmann,
Anthony J. Curcio, Chanaka De Silva, Oleg Eyser, Haixin Huang,
George J. Mahler, Dannie Steskie, and Thomas Y. Tsang
Brookhaven National Laboratory, Upton, NY, USA

[vshmakova@bnl.gov]

April 16, 2025

Abstract

Up to now, the temperatures of the carbon fiber targets used in the RHIC CNI polarimeters during proton beam interactions cannot be directly measured, yet their survival indicates that they remain below the sublimation threshold of $T_{\text{sub}} = 3915$ K. This study investigates the feasibility of using light emission as a diagnostic tool to determine the target temperatures. A dedicated optical light collection system was implemented in IP12 to capture and analyze emitted light across the visible and near-infrared spectrum. This note focuses on the initial results from the RHIC run 24 and outlines the next steps for further investigation during run 25. A proposal for an APEX run [1] was submitted as an option in case a dedicated proton beam is not available during run 25. This work is critical for assessing the applicability of carbon fiber targets in the Electron-Ion Collider (EIC) under increased beam currents.

1 Introduction

At present, the temperatures of the carbon fibers of the polarimeter targets at interaction point 12 (IP12) when bombarded by the RHIC proton beam cannot be measured directly. Obviously, the targets survive the proton bombardment and thus the carbon sublimation temperature of $T_{\text{sub}} = 3915\,\text{K}$ [2, 3] is not yet reached. This observation is consistent with an energy loss calculation using a formalism developed by Peter Thieberger at BNL[1], asuming appropriate beam sizes at the IP.

The carbon beam polarimeters have been crucial for RHIC experiments as they provide fast beam polarization measurements. Vertical and horizontal carbon fiber targets are moved through the beam to determine the corresponding polarization components p_x and p_y of the polarization vector $\vec{P} = (p_x, p_y, p_z)$ (see, e.g., Refs. [4, 5]). The carbon target width is much smaller than the beam size, allowing in addition for polarization profile measurements by moving the target through the beam, as described in Refs. [6, 7]. In view of the increased proton beam current foreseen in the Hadron Storage Ring (HSR) of the Electron-Ion Collider (EIC), it is important to establish that the carbon fiber technology is fully applicable also for polarimetry purposes at the EIC, i.e., that the carbon fibers will survive the larger beam current.

[1]Thieberger's code is available from the BNL sharepoint link at https://brookhavenlab.sharepoint.com/:x:/s/HadronPolarimetry/EQLWfFbIHvNFsF3gUfvyuNUB6NDz6HQcgJHQi0eIeXTrUw?e=F56lj0

According to the carbon temperature estimates determined using Thieberger's code[1], for the beam conditions at the future IP4 in the HSR at EIC, the target temperatures will be comparable to the ones in RHIC, despite the increased RF heating of the targets due to the use of more and shorter bunches stored in the machine. This is largely due to the beam optics in IP4 being more favorable by providing a larger beam size[2]. We emphasize that directly measuring the temperature of the carbon targets is a crucial objective and such a diagnostic tool will help to better understand the carbon target conditions during polarization measurements.

Measuring the light emitted by a hot body, on the other hand, constitutes a convenient method to directly determine the temperature of the body. The method is based on black-body radiation theory [8], which describes the spectral distribution of radiation emitted by an idealized object that absorbs all incident radiation.

A related measurement previously carried out at RHIC studied the light spectra from residual gas fluorescence and was integrated into the polarimeter setup at the HJET in IP12 [9, 10]. The system collected fluorescence light emitted by hydrogen atoms that were excited by the circulating proton beam and a fiber-coupled optical spectrometer was used to resolve the spectra. The measurement enabled a non-invasive determination of beam profiles in the horizontal plane, as described Refs. [9, 10].

2 Experimental setup

2.1 Carbon beam polarimeters

The RHIC carbon polarimeters are located at IP12. For each of the two rings (blue and yellow) a double-target chamber is installed, as shown in Fig. 1. Recoil detectors are mounted at different azimuths, as shown in panel 1a. Two target holders for vertical and horizontal fiber targets are available for each set of detectors, as shown in panel 1a. To move the target into the beam, the target holder first does a translation from its parking position near the wall of the target chamber, and then it rotates to sweep a fiber target through the beam. The target holders are made from aluminum, and each holder can support up to six fiber targets, as indicated in panel 1b.

2.2 Light detection system

2.2.1 Overview

Each of the vacuum chambers has two observation windows shown in Fig. 1a, each allowing a video camera to monitor the target movements. To collect light emitted from the target during the polarization measurement, four light collecting setups were mounted on the fused-silica glass viewports[3]. The experimental setup of the light detection system is shown in Fig. 2.

2.2.2 Light collector at the viewport

The light collector that is mounted on the fused-silica viewpoint is shown in Fig. 3. It contains the following elements:

[2]Preliminary carbon temperature estimates are given in the F. Rathmann's talk on slides 57, 59 in https://brookhavenlab.sharepoint.com/:b:/r/sites/eRHIC/bnl%26slac/EIC%20Design%20Meeting%20Minutes/Sep-11-2024/abs-had-beam-pol.pdf?csf=1&web=1&e=W7VQqB

[3]Viewport VPZL-463DU from Kurt J. Lesker Company. The viewport made of DUV fused-silica (quartz), further specifications at https://www.lesker.com/viewports/viewports-cf-flanged-quartz-fused-silica/part/vpzl-463du

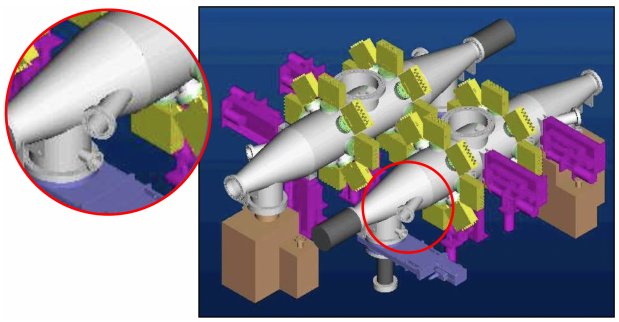

(a) Two polarimeter chambers, one for the blue and one for the yellow beam. Each chamber has two side flanges (circled in red) pointing towards the interaction region, where fused-silica viewports[3] are installed.

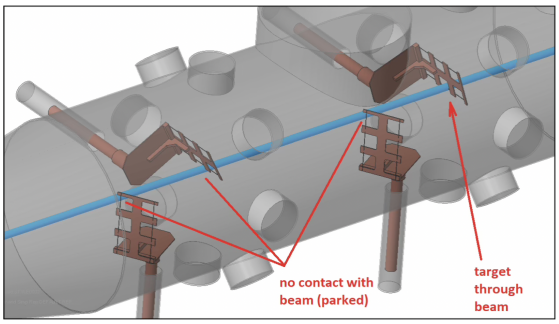

(b) Each chamber has two interaction points where the beam interacts with carbon targets that are oriented either parallel or perpendicular with respect to the ring plane, and which move either vertical or horizontal, respectively.

Figure 1: The carbon polarimeter installed at IP12 in RHIC allows for the determination of the horizontal and vertical polarization components of the beam polarization. Each chamber is equipped with two sets of up to eight silicon strip detector units [yellow boxes in panel (a)] that are used to detect carbon nuclei scattered at different azimuthal angles near $\theta_{\text{lab}} = 90°$.

1. The fused-silica ultra high vacuum viewport[3] made out of a high purity form of silica, fused silica, that has minimal absorption over a wide wavelength range. The transmission spectrum is shown in Fig. 4.

2. A Polka dot mirror[4] is an aluminum Polka dot splitter with a beamsplitting ratio of $50\% \pm 5\%$ for a beam diameter greater than 2 mm. The mirror is installed inside each light collector at a 45° angle relative to the ring plane. This allows to redirect 50% of the light upward to the collimating lens, while the remaining 50% passes through to the camera (see Fig. 2).

3. The collimator lens[6] is designed to collimate light over long distances in open air, with the ability to adjust the field of view (FOV). Its wavelength range spans from 200 to 2000 nm. The FOV was configured to produce a spot size of 1 cm at the location of the fiber target.

4. The fiberglass splitter[12] is a bifurcated optical fiber cable which is split at one end, dividing the signal into one for the visible light and one for the near-infrared light spectrometers.

2.3 Transport of light to the electronics hut in 1012

The light collected with the collimator lens is split into visible and near-infrared with the fiber splitter and transmitted further to the analyzing spectrometers in the electronics hut in the bldg. 1012 as shown in Fig. 2 with 100 m long fiberglass patch cables:

- FG200AEA[7] for transporting light of 180 - 1200 nm wavelength,
- FG200LCC[8] for signals in the range of 400 - 2200 nm.

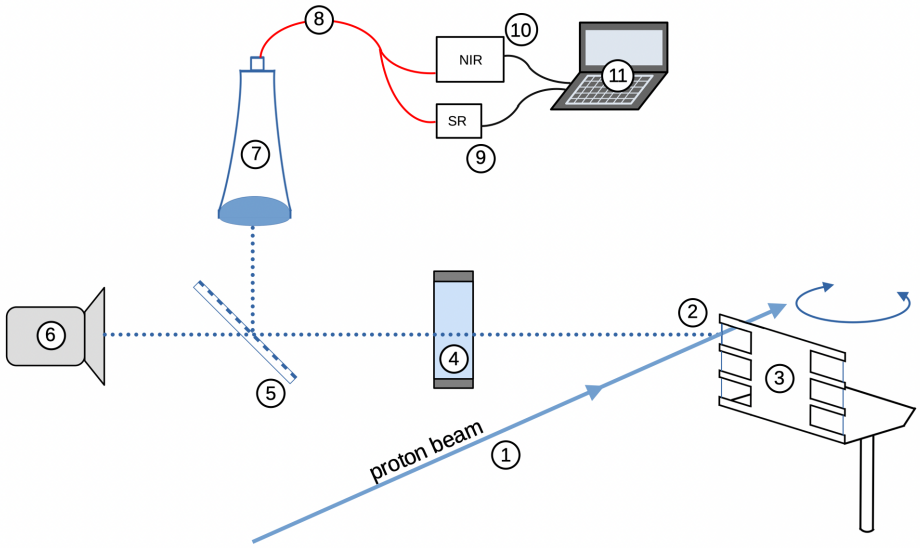

Figure 2: Schematic of the experimental setup. The fiber target (2) is secured in a holder fork (3), which rotates to move the target through the proton beam (1). The light passes through the fused-silica viewport[3] (4) and is divided by a semi-transparent Polka dot mirror[4] (5) between the video camera[5] (6) and the collimator lens[6] (7). The collimator lens is connected to the two spectrometers, SR[9] (9) and NIR[10] (10), via a splitter[12] and a fiber glass cables[7],[8] (8). Ocean View software[11] (12) is used for spectra analysis.

2.4 Spectrometer for visible light

The visible light spectrometer SR[9] is suitable for analyzing spectra in the range of 190 - 900 nm with the possibility to integrate signals over time intervals of 3.8 ms to 10 s and maximum signal to noise ratio (SNR) of 3000 : 1.

2.5 Infrared spectrometer

The near-infrared spectrometer NIR[10] analyzes infrared spectra in the range of 900 - 2200 nm with integration times ranging from 1 ms to 1 s and a SNR of 10000 : 1.

2.6 Light collection and analyzing system

The light collecting system is schematically shown in Fig. 2. Light produced by the interaction of the beam with the carbon fiber target passes via the fused-silica viewport[3] to the semi-transparent Polka dot mirror[4], where half of the light continues toward the camera, while the other half is

[4]Semi-transparent Polka dot mirror with aluminum coating pattern, made by Thorlabs, http://elog.pbn.bnl.gov:8080/uploadedMedia/1715956997515_BPD508-G-AutoCADPDF.pdf

[5]Video camera Sony, model SSC-G203A.

[6]Collimating lens 84-UV-25, made by Ocean Optics, http://elog.pbn.bnl.gov:8080/uploadedMedia/1715957132255_84-UV-25-outer-barrel.pdf

[7]Fiberglass patch cable FG200AEA, made by Thorlabs, http://elog.pbn.bnl.gov:8080/uploadedMedia/1715961542494_FG200AEA-SpecSheet.pdf

[8]Fiberglass patch cable FG200LCC, made by Thorlabs, http://elog.pbn.bnl.gov:8080/uploadedMedia/1715961343557_FG200LCC-SpecSheet.pdf

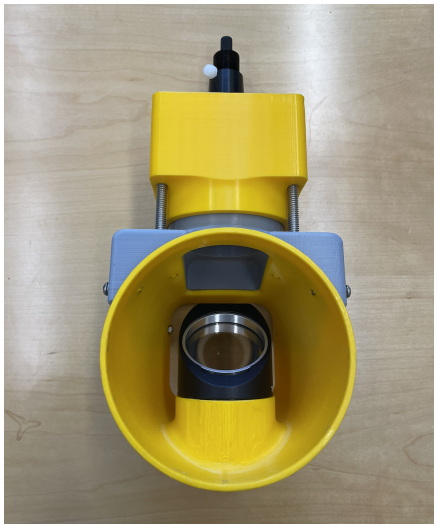

(a) View along light path onto the Polka dot mirror.

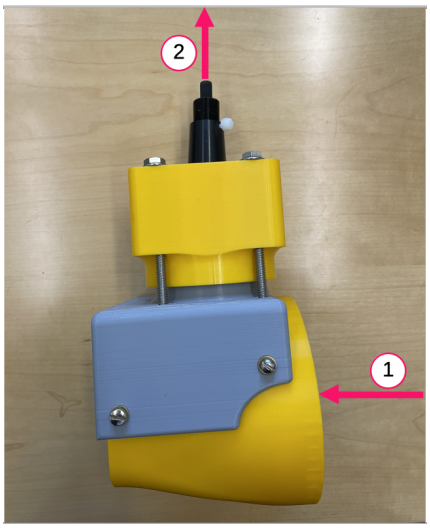

(b) Sideview, Polka dot mirror deflects light coming from the right (1) upon exiting the viewport by 90° to the collection lens, where the fiber glass cables are connected (2), which are transporting light to the spectrometers in the bldg. 1012.

Figure 3: Light collectors at the viewport. The collection lens sticks out at the top.

reflected upward by the mirror at a 90° angle into the collimator lens[6]. Light from the collimator lens is transported via a splitter[12] and fiber glass cables[7,8] to the two spectrometers in the electronic hut in the bldg. 1012. Together, the visible light (SR[9]) and the near-infrared (NIR[10]) spectrometers can analyze the spectrum across the wavelength range from 200 to 2100 nm.

3 Test measurements using an IR light source

A test setup, shown in Fig. 5, was installed in the tandem laboratory to calibrate the spectrometer response. In this setup, the experimental system (Fig. 2) was reproduced, except that the light source was replaced with a blackbody radiation oven[13], shown on Fig. 5b. The oven produces light at temperatures in the range of 50 to 1200 °C with resolution of 0.1°C. It also features various exit apertures, varying from 0.05 to 1 inch, which affect irradiance. The irradiance, which is the power emitted by a blackbody radiator through an opening and measured at the detector, is proportional to the aperture area, leading to a quadratic dependence on the aperture size.

Figure 6 shows one spectrum measured by the two spectrometers during the test measurements

[9]Visible light spectrometer SR-4UVV400-25 made by Ocean Optics, operation manual with the specifications can be found at http://elog.pbn.bnl.gov:8080/uploadedMedia/1715970344658_ocean-sr-series-installation-and-operation-manual-5-23.pdf

[10]Near-infrared spectrometer NIRQUEST+2.2-50 from Ocean Optics, operation manual with the specifications can be found at http://elog.pbn.bnl.gov:8080/uploadedMedia/1715962323489_MNL-1002-NIRQuest-UserManual-Rev-C.pdf

[11]Ocean view software https://www.oceanoptics.com/software/oceanview/

[12]Bifurcated fiberglass cable, SPLIT200-VIS-NIR, from Ocean Optics https://www.oceanoptics.com/accessories/fibers-and-probes/bifurcated-optical-fibers/mixed-uv-visible-visible-nir-bifurcated-optical-fibers

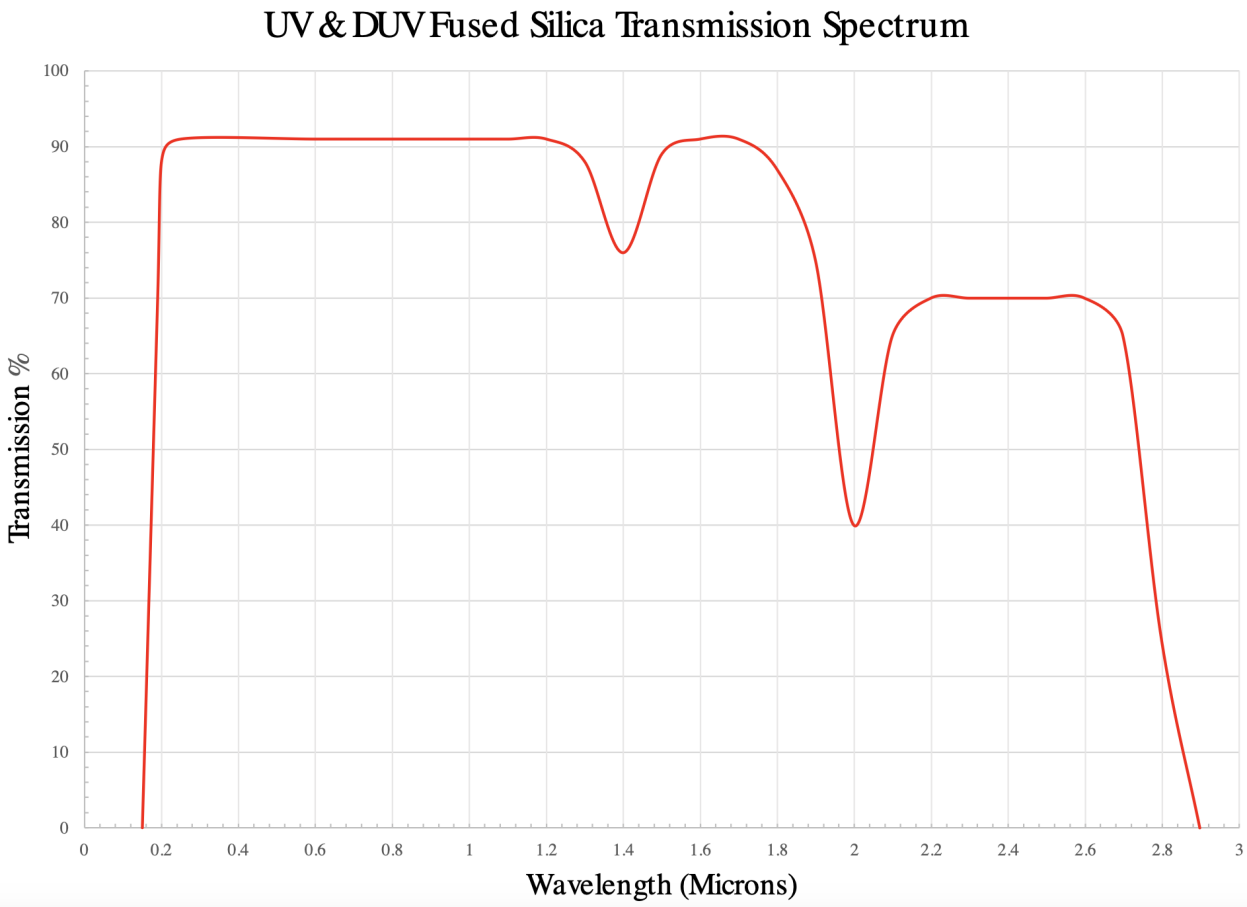

Figure 4: Fused-silica viewport transmission spectrum. The figure is taken from https://www.lesker.com/viewports/viewports-cf-flanged-quartz-fused-silica/part/vpzl-463du.

in the Van de Graaff bldg. 901A. The oven was set up to 1463 K with an aperture of 0.2 inch diameter. For comparison, several theoretical blackbody radiation spectra are included in Fig. 6. Figure 7 shows the ideal blackbody radiation spectra for different temperatures along with the wavelength ranges of the visible and NIR spectrometers.

4 First results from RHIC

During polarization measurements, the carbon fiber target moves across the beam, stops after passing through it, and then returns along the same path to its home position. Therefore, the target encounters the beam twice during each movement. The typical speed of the target motion at RHIC is 1000 to 2000 steps/s, depending on the target size and the beam intensity, where 700 steps = 1 mm. Data collection was continuous over approximately two weeks, with an integration time of 1 second for both the SR and NIR spectrometers. During this period, polarization measurements were typically conducted two to five times per day. The timing information from measurements with the Y1 target, where the light collection system was installed, was used to identify and select

[13] Infrared light source IR-574/301, made by Infrared Systems Development Corporation. See manual at http://elog.pbn.bnl.gov:8080/uploadedMedia/1715969781515_Manuals_F_FUR1270_A.pdf

(a) The oven emits light into the viewport, which is housed in the yellow holder. Inside the holder, a Polka dot mirror reflects the light upward to the collimation lens. Fiber optic cables connect the lens to the spectrometers.

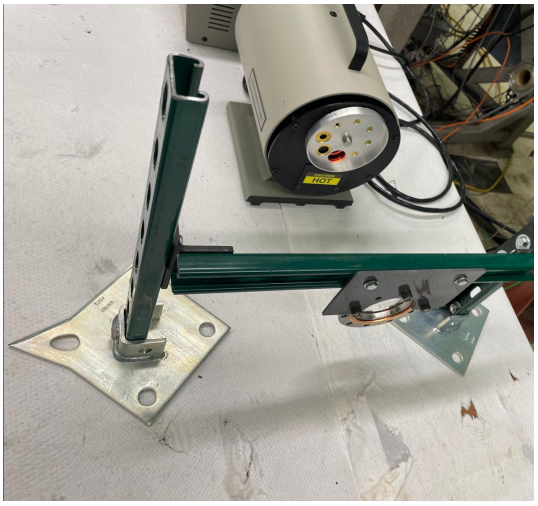

(b) The blackbody radiation oven[13] has multiple aperture openings available.

Figure 5: The test setup in the Tandem laboratory.

the relevant signal spectra.

The background was estimated using spectra recorded over a 20-second period starting at $t_m - 80\,\mathrm{s}$, where t_m is the time of the polarization measurement. Since, for one polarization measurement, the target was moved through the beam twice, once in the forward direction and once in reverse, this motion pattern was observed using the NIR spectrometer, which recorded a clear but small signal each time the target crossed the beam, as shown in Fig. 8. The recorded signal represents the intensity after subtracting the background. The observed peak signal is located at approximately 1600 nm, which coincidentally aligns closely with the test measurement of blackbody radiation at 1463 K, as shown in Fig. 6. The lower-than-expected temperature, along with the small signal amplitude, indicates that the light collecting system was not aligned precisely enough. As a result, we were obviously missing the light from the center of the target that directly interacts with the beam. Since the pC polarimeter chambers were already closed and pumped down during the alignment work, optimal lens alignment was not possible anymore. This will be the main item that we are going to improve for run 25 – ensuring proper alignment with an open chamber to make sure we are able to collect light from the target region.

4.1 Trigger development

The Polarimeter Trigger Manager was developed to provide a reliable and automated method for synchronizing spectrometer data collection with polarimeter target motion, ensuring efficient data acquisition.

Spectrometer data could be acquired by an external trigger pulse. The spectrometers and the windows laptop which hosted the spectrometer software are located in the electronic hut in 1012. Fiber cables were run from the RHIC tunnel into the computing room. We used two delay channels coming from the delay channel *cfe-12a-polar1* for spectrometer triggering purposes. The manager logic was developed to issue triggers based on polarimeter target motion during measurements

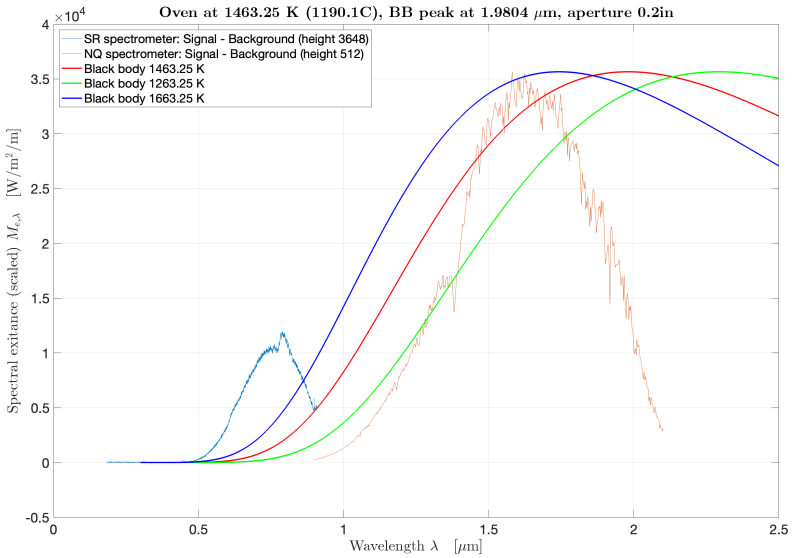

Figure 6: Measured spectra of black body radiation simulated by the oven at 1463 K. The SR spectrometer covers a wavelength range of 0.2 to 0.9 μm, while the NIR spectrometer covers 0.9 to 2.1 μm. The measured spectrum ais compared to the theoretical blackbody radiation spectra at 1463.25 K, 1263.25 K, and 1663.25 K.

performed by the MCR.

The efforts were coordinated between experimenters, controls hardware and controls software. The experimenters provided relevant specs needed for spectrometer trigger cable interfacing. Controls hardware helped with identifying which front end to use for getting trigger signals, running trigger cables and making customized cable terminations at the spectrometer end.

4.1.1 Requirements

The system had to provide a stream of triggers at a regular frequency to the data acquisition equipment only while the polarimeter target is moving. A trigger frequency in the neighborhood of 1 Hz is acceptable. Note that control system delay channel triggers can be configured to trigger at regular frequencies by delaying triggers from any of the regularly occurring events on the RHIC event link (720hz, 60hz, 10hz, 1hz, 25hz). No custom software is needed for that functionality. The custom manager software is needed to turn triggers on when target motion starts and off when target motion stops.

4.1.2 Design and Implementation

Two delay channels in *cfe-12a-polar1* (*delayChannel.12a-polar1.A0*, *delayChannel.12a-polar1.A1*) were assigned to provide the triggers. Using pet interface, experimenters were able to adjust the trigger pulse period and duty cycle to determine the best pulse properties for acquiring and saving light spectrum data.

PolarTargetMan software monitors the *movingM* parameter in the *pol.y-vtarget* and *pol.y-htarget* automated device objects (ADOs) to detect target motion.

- If target motion is detected (*movingM*!=0) for either of the two targets and the two delay

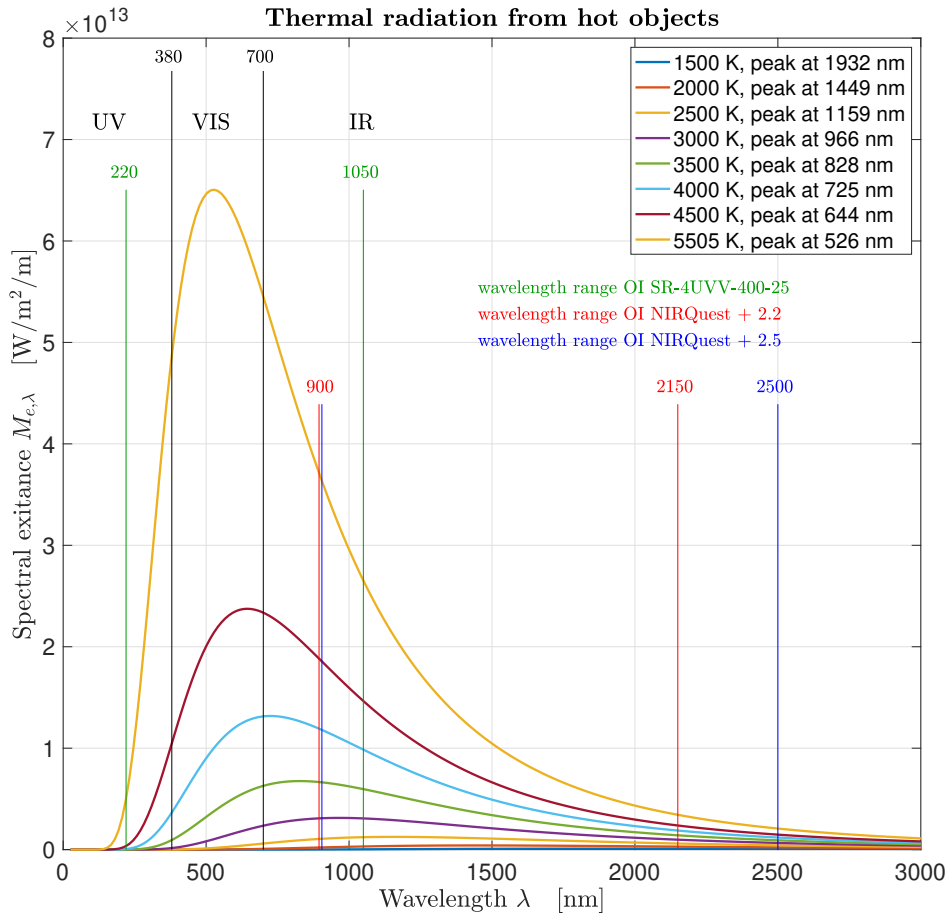

Figure 7: Black body radiation spectra depending on temperature. Green lines mark the wavelength range of the SR visible light spectrometer[9], while red lines indicate the range for the NIR spectrometer[10].

channels are both in an "Off" state, the manager sends "On" to the *holdS* parameter for both delay channels.

- If both targets are detected to have stopped (*movingM*==0) and the two delay channels are both in an "On" state, the manager sends "Off" to the *holdS* parameter for both delay channels.

5 Conclusion

This study investigates the temperature of carbon fiber targets used in the RHIC CNI polarimeters during proton polarization measurements. Because direct temperature measurements of the targets are not yet possible, an optical system was implemented to collect and analyze light emissions in the visible and near-infrared spectrum. Test calibrations were conducted using a blackbody radiation source, and initial RHIC measurements in run 24 revealed a weak signal roughly corresponding to a heating of 1400 K. The low signal intensity is traced to a misalignment of the collimating lens, causing the light collection from a cooler, darker region off-center from the fiber target.

The collimating lens detects light from a circular area with a certain finite radius, which means

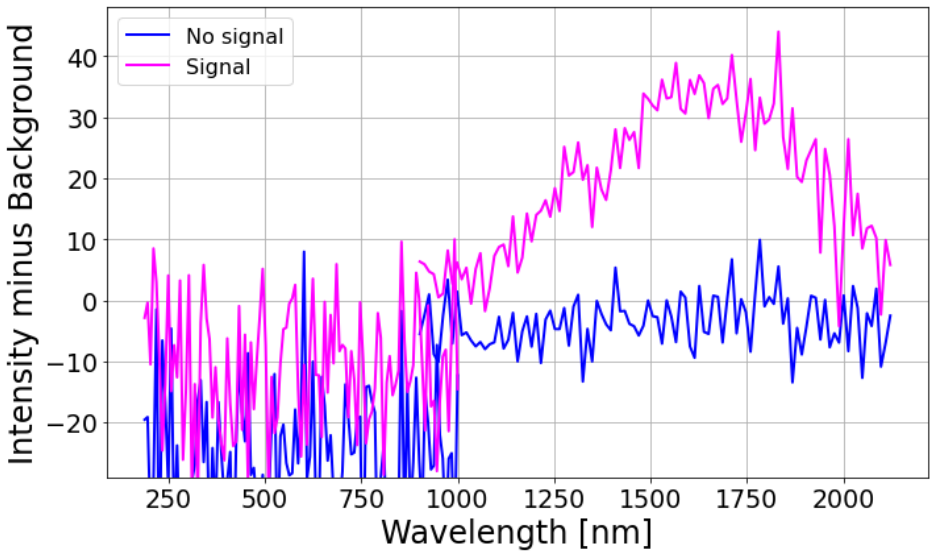

Figure 8: Signal observed during target movement through the beam shown in magenta. Blue line shows spectra before the target movement.

that the signal from the target center is mixed with signals from other, cooler parts of the fiber and from the background material of the target holder. This mixing distorts the observed blackbody radiation spectrum. To correct for this effect, a Monte Carlo simulation should be performed using a model of the temperature distribution along the fiber, adjusting for different lens acceptance spot sizes, plus includes background from the walls of the vacuum chamber.

During the RHIC run 24, the alignment was not precise enough and the collimating lens was not collecting light from the center part of the target. Additionally, the measured temperature of approximately 1400 K is lower than expected, which is consistent with the conclusion. To ensure accurate data collection in run 25, proper alignment of the collimating lens is essential.

5.1 Outlook

It is understood that during run 25, dedicated proton beam, if available, will only be available in the blue ring, as the forward STAR detector was upgraded and it requires protons moving clockwise (i.e., in blue ring) for forward scattering. Gold beams cannot be used on the targets because, as shown in Appendix A, their energy loss is significantly higher than that of protons. This makes the carbon fiber target unsustainable under gold beam conditions. As a result, two new light collectors on the viewports B1 and B2 need to be installed on the blue ring, with the capability to collect signals from both viewports simultaneously.

5.1.1 Viewport hardware improvements

During run 24, mounting the viewport holders required forcing them onto the flanges, which was not ideal and compromised precise alignment perpendicular to the ring plane.

For run 25, redesigned holders have been developed. They feature a larger entrance diameter than the flange and include a built-in step for easy placement without force. They will be secured with fixation screws, and their interior surface will be covered with black felt to prevent light reflections inside the light collectors.

5.1.2 Optical alignment

To improve alignment, a visual crosshair target (shown in Fig. 9a) will be mounted at the intersection of the fiber target and the beam. A laser beam will be directed through the collimating lens, as shown in Fig. 10, and the lens orientation will be adjusted until the laser spot aligns with the center of the crosshair. This procedure will be performed for both vertical and horizontal targets at viewports B1 and B2. Additional effort is needed to focus the video camera on the target to obtain a clear image during the measurement.

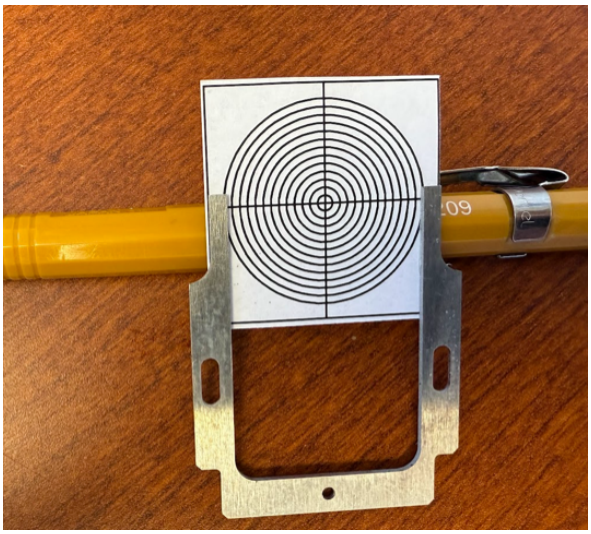

(a) Crosshair visual target in a target holder.

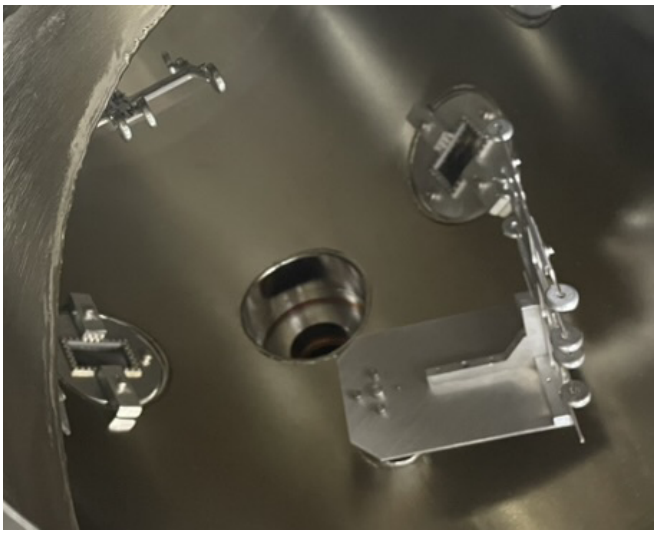

(b) View on a target holder fork inside a CNI polarimeter vacuum chamber.

Figure 9

5.1.3 Target temperature monitoring

To monitor temperature of the target holder when heated by the beam – important piece of information – a UHV-compatible PT100 resistance thermometer could be mounted on one of the holders. Each target station has eight detector flanges, with only six currently used for detectors. The unused flange at the bottom, as illustrated in Fig. 9b, could be used for a feedthrough to route the sensor connection. However, due to scheduling changes prior to the run, this idea had to be abandoned.

5.1.4 Run 25 beam availability

However, the availability of a dedicated proton beam for run 25 remains uncertain. To prepare for this possibility, an APEX proposal [1] has been submitted, requesting 100 GeV stored protons with the maximum number of bunches in the blue ring, in case there will be no dedicated proton beam operation during run 25.

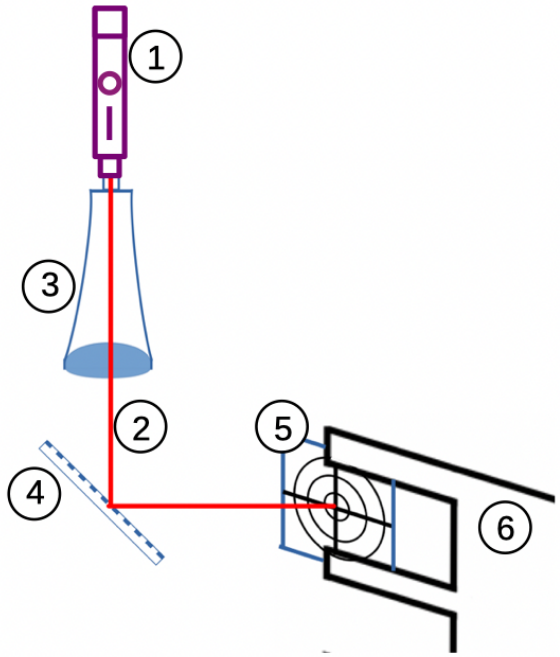

Figure 10: Alignment scheme. Laser pointer (1) feeding light (2) in the collimator lens (3). Light is reflected by a Polka dot mirror (4) in the direction of the crosshair target (5) fixed in the fiber target holder (6). Orientation of the lens can be adjusted that laser spot aligned with the crosshair center.

A Energy loss in C targets

Discussion of energy loss in C target for proton and Au beam at the same kinetic energy per nucleon using the Bethe-Bloch formalism.

A.1 Bethe-Bloch formalism

The Bethe-Bloch formula [11] for energy loss is given by

$$-\frac{dE}{dx} = 2\pi N_A r_e^2 m_e c^2 \frac{Z}{A}\frac{z^2}{\beta^2}\left[\ln\left(\frac{2m_e\gamma^2 v^2 W_{\max}}{I^2}\right) - 2\beta^2\right] \tag{1}$$

where:

The conversion from stopping power $\frac{dE}{dx}$ in units of MeV/cm to MeV/(g/cm^2), also known as the *mass stopping power*, the following formula is used,

$$\left(\frac{dE}{dx}\right)_{\text{mass}} = \frac{1}{\rho}\left(\frac{dE}{dx}\right), \tag{2}$$

where $\frac{dE}{dx}$ is the stopping power in MeV/cm, ρ is the density of the material in g/cm^3, and $\left(\frac{dE}{dx}\right)_{\text{mass}}$ is the mass stopping power in MeV/(g/cm^2).

Symbol	Description
N_A	Avogadro's number (6.022×10^{23} mol^{-1})
r_e	Classical electron radius (2.817×10^{-13} cm)
m_e	Electron mass
c	Speed of light
Z	Atomic number of absorbing material
A	Atomic weight of absorbing material
ρ	Density of absorbing material
z	Charge of incident particle in units of e
$\beta = \frac{v}{c}$	Velocity of the incident particle relative to c
$\gamma = \frac{1}{\sqrt{1-\beta^2}}$	Lorentz factor
I	Mean excitation potential
$W_{\max}$	Maximum energy transfer in a single collision

The total energy loss ΔE over a path length can be expressed in integral form as

$$\Delta E = \int_{x_1}^{x_2} \frac{dE}{dx}\, dx\,, \tag{3}$$

where x_1 and x_2 are the starting and ending points of the path, $\frac{dE}{dx}$ is the stopping power, which may depend on x or other variables like particle energy. Using the mass stopping power $\left(\frac{dE}{dx}\right)_{\text{mass}}$ with material density ρ, then

$$\Delta E = \int_{x_1}^{x_2} \left(\frac{dE}{dx}\right)_{\text{mass}} \cdot \rho\, dx \tag{4}$$

A.2 Comparison of proton and Au beams

In the following comparison, it is assumed that each of the impinging protons contained in a Au nucleus hitting the C target has the *same* kinetic energy of 100 GeV per nucleon as the corresponding proton beam. Thus the kinematic parameters β and the Lorentz factor γ are the same in the two cases.

A.2.1 p+C scattering

For protons impinging on carbon, the relevant factor is

$$\frac{Z(\text{C})}{A(\text{C})} \cdot z(p)^2 = \frac{6}{12} \cdot 1^2 = 0.5 \tag{5}$$

A.2.2 Au+C scattering

For Au, the situation is given by

$$\frac{Z(\text{C})}{A(\text{C})} \cdot z(\text{Au})^2 = \frac{6}{12} \cdot 79^2 = 3120.5 \tag{6}$$

A.3 Conclusion

Even if the number of Au nuclei in a RHIC bunch is 100× smaller than with protons, the total energy loss for Au in the C targets will be still ≈ 60 times larger than for protons, and the C targets will not survive the Au beam.

References

[1] F. Rathmann et al., "Light from carbon targets," (2025), URL https://www.c-ad.bnl.gov/BeamEx/details.asp?index=559.

[2] Wikipedia contributors, "Carbon," (2025), accessed: 2025-01-15, URL https://en.wikipedia.org/wiki/Carbon.

[3] W. M. Haynes, D. R. Lide, and T. J. Bruno, *CRC Handbook of Chemistry and Physics* (CRC Press, Boca Raton, FL, 2016), 97th ed., ISBN 978-1-4987-5429-3.

[4] H. Huang et al., "Commissioning of RHIC p carbon CNI polarimeter," Nucl. Phys. A **721**, 356 (2003).

[5] H. Huang, in *Beam Instrumentation Workshop 2000: Ninth Workshop* (AIP, 2000), vol. 546 of *American Institute of Physics Conference Series*, pp. 440–447.

[6] W. Fischer and A. Bazilevsky, "Impact of three-dimensional polarization profiles on spin-dependent measurements in colliding beam experiments," Phys. Rev. ST Accel. Beams **15**, 041001 (2012), URL https://link.aps.org/doi/10.1103/PhysRevSTAB.15.041001.

[7] A. Zelenski et al., "The RHIC p-carbon CNI polarimeter upgrade for the beam polarization and intensity measurements," AIP Conf. Proc. **1149**, 731 (2009).

[8] M. Planck, *The Theory of Heat Radiation* (P. Blakiston's Son & Co., 1914).

[9] T. Tsang, S. Bellavia, R. Connolly, D. Gassner, Y. Makdisi, M. Minty, T. Russo, P. Thieberger, D. Trbojevic, and A. Zelenski, in *Particle Accelerator Conference (PAC 09)* (2010), p. TH5RFP019.

[10] T. Tsang, D. Gassner, and M. Minty, "Residual gas fluorescence monitor for relativistic heavy ions at RHIC," Phys. Rev. ST Accel. Beams **16**, 102802 (2013).

[11] W. R. Leo, *Techniques for Nuclear and Particle Physics Experiments: A How to Approach* (1987), ISBN 978-3-540-57280-0.